Laser Amplifier Development for the Remote Sensing of CO_2 from Space

Anthony W. Yu *[a], James B. Abshire [a], Mark Storm [b], Alexander Betin [c]
[a] NASA Goddard Space Flight Center, Greenbelt MD USA 20771;
[b] Fibertek, Herndon VA 20171;
[c] Raytheon Space and Airborne Systems, El Segundo, CA, USA 90245

ABSTRACT

Accurate global measurements of tropospheric CO_2 mixing ratios are needed to study CO_2 emissions and CO_2 exchange with the land and oceans. NASA Goddard Space Flight Center (GSFC) is developing a pulsed lidar approach for an integrated path differential absorption (IPDA) lidar to allow global measurements of atmospheric CO_2 column densities from space. Our group has developed, and successfully flown, an airborne pulsed lidar instrument that uses two tunable pulsed laser transmitters allowing simultaneous measurement of a single CO_2 absorption line in the 1570 nm band, absorption of an O_2 line pair in the oxygen A-band (765 nm), range, and atmospheric backscatter profiles in the same path. Both lasers are pulsed at 10 kHz, and the two absorption line regions are sampled at typically a 300 Hz rate.

A space-based version of this lidar must have a much larger lidar power-area product due to the ~x40 longer range and faster along track velocity compared to airborne instrument. Initial link budget analysis indicated that for a 400 km orbit, a 1.5 m diameter telescope and a 10 second integration time, a ~2 mJ laser energy is required to attain the precision needed for each measurement. To meet this energy requirement, we have pursued parallel power scaling efforts to enable space-based lidar measurement of CO_2 concentrations. These included a multiple aperture approach consists of multi-element large mode area fiber amplifiers and a single-aperture approach consists of a multi-pass Er:Yb:Phosphate glass based planar waveguide amplifier (PWA). In this paper we will present our laser amplifier design approaches and preliminary results.

Keywords: lidar, laser spectroscopy, solid-state laser amplifier, space laser transmitter, fiber amplifier

1. INTRODUCTION

We are conducting research on a laser sounder instrument for global (Earth and Mars) measurements and profiling of atmospheric CO_2 in support of the future Active Sensing of CO_2 Emissions over Nights, Days, and Seasons (ASCENDS) mission.[1] Although increasing atmospheric CO_2 is widely accepted as the largest anthropogenic factor causing climate change, there is considerable uncertainty about its global budget. Accurate measurements of tropospheric CO_2 mixing ratios are needed to study CO_2 emissions and CO_2 exchange with the land and oceans. To be useful in reducing uncertainties about carbon sources and sinks the atmospheric CO_2 measurements need degree-level spatial resolution and ~ 0.3% precision. Our group has developed a pulsed lidar approach as a candidate for the ASCENDS mission (Figure 1).[2,3] Our approach uses an erbium doped fiber amplifier (EDFA) based transmitter for atmospheric CO_2 measurements in an overtone band near 1572 nm.[4] It uses a dual band pulsed laser absorption spectrometer and the integrated path differential absorption (IPDA) or the laser sounder technique.[5] The approach uses two tunable pulsed laser transmitters allowing simultaneous measurement of the absorption from a CO_2 absorption line in the 1570 nm band, O_2 absorption in the oxygen A-band (765 nm), and surface height and atmospheric backscatter in the same path. A tunable laser is stepped in wavelength across a single CO_2 line for the CO_2 column measurement, while simultaneously a laser is stepped across a line doublet near 765 nm in the Oxygen A-band for an atmospheric pressure measurement.[6,7] Both lasers are pulsed at a ~8 kHz rate, and the two absorption line regions are sampled at each wavelength step at typically ~1 kHz. The direct detection receiver measures the time resolved laser backscatter from the atmosphere along with the energies of the laser echoes from the surface. After suitable averaging the gas extinction and column densities for the CO_2 and O_2 gases are calculated from the sampled wavelengths of the surface reflected line shapes via the IPDA lidar technique.[8]

For the ASCENDS instrument, the wavelength stability and tunability requirement for sampling the absorption feature of the CO_2 and O_2 gases drove the laser transmitter to a MOPA architecture. We have recently demonstrated a wavelength-locked laser source that rapidly steps through six wavelengths distributed across a 1572.335 nm CO_2 absorption line to allow precise measurements of atmospheric CO_2 absorption. A similar approach will be used for the 1529 nm wavelength band and then frequency doubled to generate the 764.5 nm for oxygen sensing.

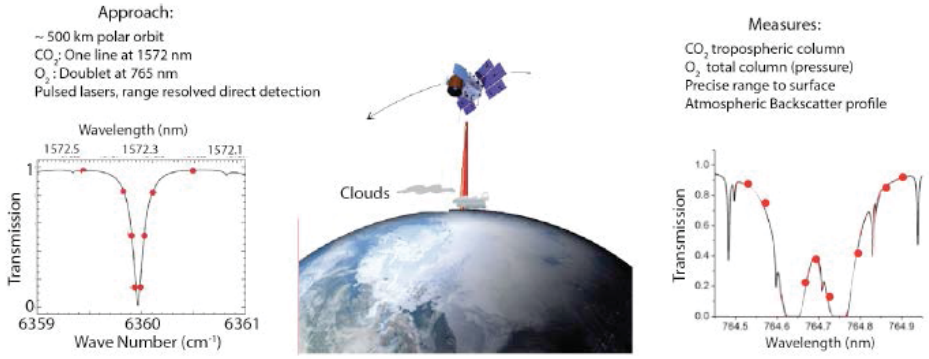

Figure 1. Our CO_2 Laser Sounder approach, which measures the column CO_2 & O_2 absorption and range to the scattering surface from space. (Left) Nominal CO_2 line (1572.33 nm) targeted for use for 2-way pass to surface from space. The laser sounder measures the shape and depth of this CO_2 line and the absorption of a line doublet near 764.7 nm in the O_2 A-band (Right). The line sampling approach is flexible and we plan 8-wavelength samples/line.

We have also, over the past few years, successfully flown several airborne campaigns demonstrating the measurement concepts and verified our link model.[9,10,11] To scale for space, the energy per pulse in each of these wavelengths (1529 nm and 1572 nm) needs to be increased to appropriate levels. A space-based version of this lidar must have a much larger lidar power-area product due to the ~x40 longer range and faster along track velocity compared to airborne instrument (see Figure 2). We have developed receiver SNR models for both the CO_2 and O_2 channels and applied them to estimate lidar parameters needed for the space measurement (see Table 1). Initial calculations indicated that for a 500 km orbit, a 1.5 m diameter telescope and a 10 second integration time, which allows a 70 km along track integration in low earth orbit, a ~2 mJ laser energy is required to attain the precision needed for each measurement. The instrument power consumption is between 600 and 900W depending on the detector sensitivity. An initial mass estimate is 400 kg, and the uncompressed data rate is < 2 Mbits/sec.

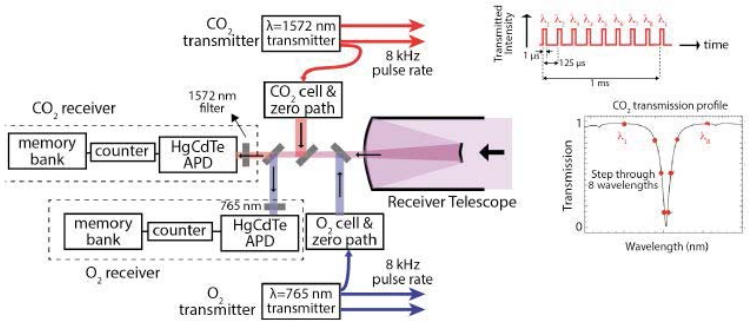

Figure 2. Block diagram of the space lidar instrument. Simultaneous measurements are made of CO_2, and O_2, absorption line shapes, time of flight, and backscatter profiles at 1572.33 nm and 764.7 nm wavelengths. The return light is collected by a common 1.2-m telescope and detected.

Table 1. The derived laser transmitter requirements are summarized here. The requirements were based on feedback from airborne campaigns and link budget analysis.

Performance Parameter	Laser Transmitter Overall Performance
Center Wavelength	1572.335 nm and 1529 nm
Tuning speed	NA
Linewidth	≤ 100 MHz
Side-mode suppression ratio (spectral)	>30 dB
Pulse repetition frequency	7.5 KHz
Pulse period (derived)	133 μs
Pulse Width	100 ns – 1 μs (assume 1 μs)
Duty Cycle (derived)	0.75 %
Pulse shape	Trapezoidal
Pulse energy	>3.2 mJ (goal); >2.5 mJ (operating)
Average power (informational derived)	>24 W (goal); 20 W (operating)
Peak power	3.2 KW goal; 2.5 kW operating
PER [TBR]	20 dB
Wall-plug Efficiency	> 10% (goal)

2. LASER TRANSMITTER

2.1 Laser Architecture

The space-based lidar instrument concept uses a master oscillator power amplifier (MOPA) approach for the laser. The MOPA laser consists of a tunable diode master oscillator seed lasers and two stage power amplifiers. This modular approach is flexible and has a number of advantages. A key one is that it leverages the lower power stages we have already demonstrated and scales to space by adding power amplifiers to them. The diode seed lasers for the CO_2 and O_2 wavelengths are highly developed, and have been space qualified. To meet the precision, the online lasers need to be frequency stabilized to ~1 MHz.[12] We have locked the master laser diode to the CO_2 line center and achieved frequency drifts < 0.3 MHz over 72 hours. We have demonstrated a new step-locked single laser diode source that accurately locks its output to 8 or more wavelengths around the CO_2 absorption line. This allows a significant simplification to the seed laser stage.

The laser sounder for Earth atmospheric CO_2 requires measurements of atmospheric O_2 (pressure and temperature). The ratio of CO_2 to O_2 will provide a measurement of the dry-air mixing ratio of CO_2. This quantity should be insensitive to fluctuations in surface pressure resulting from changing topography or weather systems and to fluctuations in temperature and humidity. For O_2, the most straightforward approach is a 1540 nm DFB-laser-diode oscillator frequency-doubled erbium-fiber-amplifier (1540nm/770nm) MOPA transmitter.[13] More recently we have achieved over 1 kW peak power from a 1530 nm fiber amplifier.[14]

2.2 Master Oscillator

A distributed-feedback laser diode (DFB-LD) was frequency-locked to the CO_2 line center by using a frequency modulation technique, limiting its peak-to-peak frequency drift to 0.3MHz at 0.8 s averaging time over 72 hours.[15] Four online DFB-LDs were then offset locked to this laser using phase-locked loops, retaining virtually the same absolute frequency stability.[16] These online and two offline DFB-LDs were subsequently amplitude switched and combined. This produced a precise wavelength stepped laser pulse train, to be amplified for CO_2 measurements.[17] Figure 3 shows a conceptual master oscillator approach.

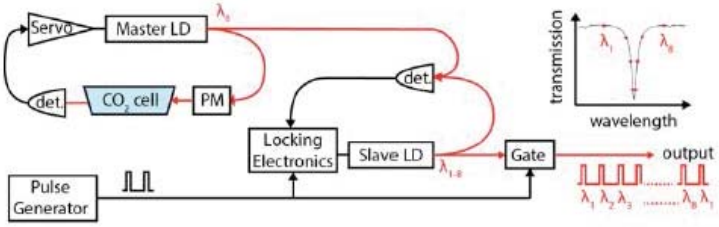

Figure 3. Schematic of a stepped wavelength locked source, as demonstrated in [31]. The master wavelength is locked to a CO_2 absorption cell. By offset-locking a slave laser at different frequency offsets to the master, we generate a pulse train step-locked 8 discrete points on 1572.335 nm CO_2 line.

2.3 Power Amplifier Approaches

2.3.1 Single Aperture Approach – Er:Yb:Phosphate Planar Waveguide Amplifier

We are pursuing a single power amplifier (PA) approach led by Raytheon Space and Airborne Systems (RSAS) to meet the energy requirement for the CO_2 and O_2 sensing from space. The seed laser input for this approach is the laser transmitter from our airborne lidar that uses a commercial EDFA as a preamplifier and produces pulse energy of 25 µJ, pulse width of 1 µsec with 25 W peak power, or 0.25 W average power. The approach for the amplifier for both wavelengths is shown in Figure 12, which uses a custom Er:Yb:Phosphate planar waveguide amplifier (PWA) PA proceeded by a fiber pre-amplifier. In our previous effort with RSAS, they have successfully produced and demonstrated the advantages of PWA for swath mapping application.[18] The scaling for CO_2 and O_2 sensing at the 1572 and 1529 nm bands requires careful selection of material and efficient amplifier design since these wavelength bands of interests are on either end of typical erbium glass gain spectrum. Appropriate pump and gain confinement are needed in

a reasonably sized package for space deployment. The erbium doped phosphate glass is chosen because it provides a broad gain spectrum, and Yb:Er co-doping allows using space qualified 940nm pump diode modules.[19] More importantly, the planar waveguide (PWG) concept, which is based on Raytheon's proprietary technology, is chosen for its advantages of efficient gain confinement and thermal management.[20]

The overall schematic of the MOPA laser is shown in Figure 4 and the output energies and efficiencies calculated from RSAS's laser amplifier model are summarized in Table 2. Figure 5 illustrates the generic PWG design. The PWG is essentially a flat fiber in which the core is index-guided in one dimension and unguided in the other wide dimension. The signal is mode matched into the core that has a typical dimension of 50–200μm. The high aspect ratio of the PWG design provides a large surface area for efficient cooling that can be managed with conventional cooling mechanisms. In our architecture, the PWG will be cladding pumped by power combining three 940 nm pump laser diode arrays.

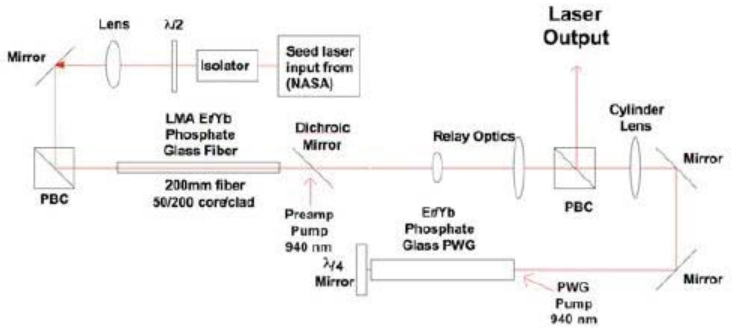

Figure 4. Schematic of the MOPA laser transmitter consists of multi-pass planar waveguide amplifier approach for power scaling.

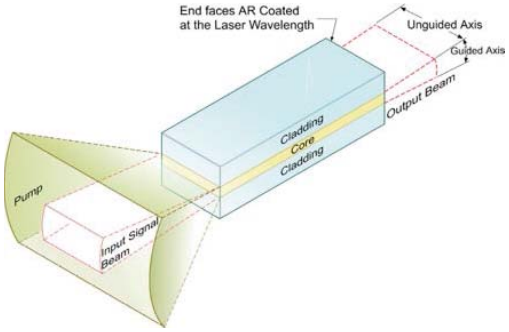

Figure 5. Typical planar waveguide structure.

Table 2. Modeling results of PWG performance at different wavelengths for CO2 and O_2 sensing.

Wavelength	PWG Pump Power @ 3mJ Output Energy	Efficiency @ 3mJ Output Energy	Max PWG Pump Power	PWG Output Energy @ Max Pump	Efficiency @ Max Pump Power *
= 1569 nm	170W	8.4%	400 W	8.7 mJ	10.3%
= 1572 nm	190 W	7.5%	400 W	6.7 mJ	8.0%
= 1575 nm	240 W	6.0%	400 W	4.2 mJ	5.0%
= 1529.6 nm	160 W	9.0%	400 W	7.3 mJ	8.7%

RSAS is completing the development of a four-pass PWG-based power amplifier breadboard shown in Figure 6. The PWG PA is ~150mm long Er:Yb:phosphate planar waveguide with overall cross section dimension of 0.5 mm (T) x 5 mm (wide). The wall-plug efficiency will be ~8%. RSAS is in the process of assembling a breadboard of this Er:Yb:Glass PWG-based laser amplifier and evaluate its capabilities. Several planar waveguides (PWG) designs have already been fabricated and delivered for early evaluation.

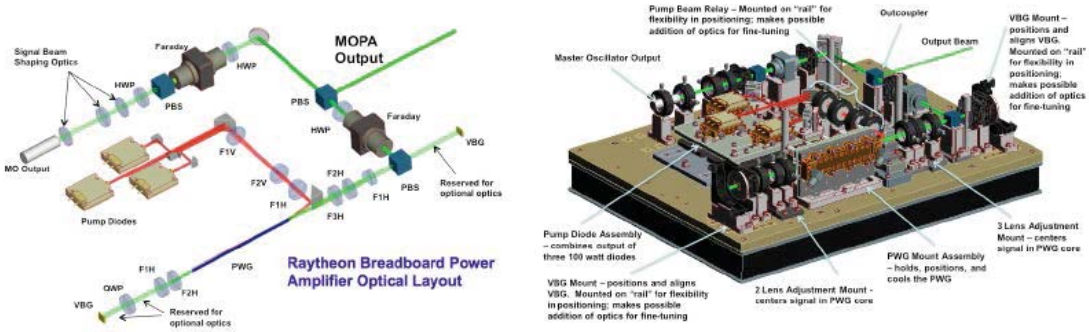

Figure 6. (Left) Optical beam path of the multi-pass PWA that is being assembled. The PWG is pumped by three 940 nm laser diodes. Narrow band mirrors using volume Bragg gratings (VBGs) are used to reject out of band ASE and gain. (Right) CAD of the breadboard PA for the optical layout on the left. The overall dimension is 24"x18"x2.5".

The fabrication and manufacturing processes of crystalline-based PWGs have been matured and successfully delivered and demonstrated. However, the manufacturing process of glass based PWG is still being refined. Several Er:Yb:Phosphate glass PWGs have been fabricated that have the correct core thickness but varying cladding thicknesses have been assembled and being evaluated at RSAS (see Figure 7).

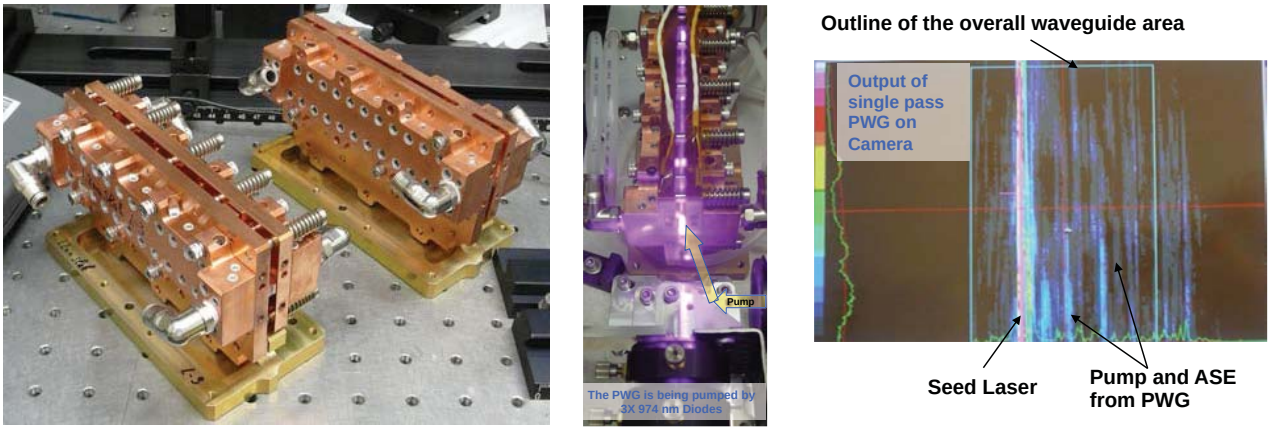

(a) (b) (c)

Figure 7. (a) Assembled PWGs, sandwiched between two water-cooled heat sinks and spring loaded mechanical mount for efficient thermal management; (b) One of the assembled PWG modules is being pumped by 940 nm pump diodes; (c) A beam profiling camera capturing the seed laser, unabsorbed pump light and amplified spontaneous emission (ASE) from the PWG module shown in (b). The green line outlines the dimension of the overall PWG.

Initial evaluation has confirmed that the cladding thicknesses played a significant role in pump confinement, which leads to how efficient pump light will be absorbed by the gain medium and leakage of unabsorbed pump out of the PWG. The PWGs that are fabricated to meet our designed dimensions are close to completion. We will report the performance of this power amplifier in the near future.

2.3.2 Multi Aperture Approach – Large Core Fiber Amplifiers

The goal of this effort is to provide a compact, efficient, and high-energy all-fiber lidar transmitter that will meet the ASCENDS requirements with a straightforward path to a space flight system. The system design is based on an advanced, eye-safe, polarization-maintaining (PM) MOPA lidar transmitter platform that was under development at Fibertek. This platform consists of a narrow linewidth (400 Hz - 1MHz) and highly stable seed laser, a flexible and reconfigurable pulse generator, and multiple stages of PM Erbium doped fiber amplifiers with increasing mode-field area. Using this architecture, we have demonstrated up to 475 µJ energy per pulse at 1572.3 nm, and up to 250 µJ energy per pulse at 1529 nm wavelength with 1.5 µs pulse width and 10 kHz repetition rate. The output beams at the highest energy levels were diffraction limited, and the polarization extinction ratio (PER) was ~17dB. The optical to optical conversion efficiency was ~17% with respect to total pump power.

2.3.2.1 CO_2 Channel – Power Scaling of 1572 nm

To satisfy the overall mission goal of ~2 mJ per pulse energy as shown in Table 1, multiple fiber amplifiers will be incoherently combined to provide the required energy in the far field for lidar measurement. All of the power amplifier chains will be seeded from the same seed laser. A prototype fiber amplifier breadboard based an all-fiber MOPA architecture was built and tested with PM fiber components and operated in single transverse mode. The obtained energy levels at 1572.3 nm at each stage are illustrated in Figure 8.

In this test, the master oscillator (MO) was a DFB-LD, with a center wavelength of ~1571.2 nm (25 ºC, 100mA), and output power of up to 50 mW. The center wavelength was shifted to the desired CO_2 absorption band of 1572.3 nm by appropriately adjusting the DFB-LD's temperature and bias current. The MO was operated in continuous-wave (CW) mode for our system for best wavelength stability and narrowest linewidth of <1 MHz. The output average power of the DFB laser was ~15 mW.

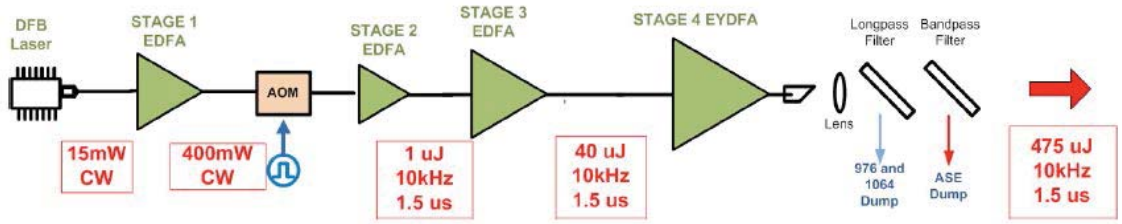

Figure 8. Experimental setup with illustrated 1572.3 nm power/energy levels at each stage.

The first stage of amplification is placed before the pulse carving stage, in order to provide the highest energy to the subsequent amplifier stages. At the 1570nm band, the gain of the EDFA is lower, so saturation becomes extremely important to achieve the lowest amplified spontaneous emission (ASE) noise. The stage 1 EDFA is built with ~15 meters of Er/Yb co-doped PM single-mode fiber that is widely used in telecom systems. It has core and cladding diameters of 7 μm and 125 μm, and pumped with a broad area laser diode at 976 nm. The amplifier has an 18 nm bandpass filter, centered at 1570 nm at the output. A sample output spectrum at 80 mW CW power (at 2.5A pump current) is shown in Figure 6. This amplifier could be operated up to ~400 mW which is the damage threshold of the output isolator.

Pulse carving at 10 kHz from the amplified CW signal is achieved by using an acousto-optic modulator (AOM). The AOM is chosen mainly for two purposes: high extinction ratio (~47 dB) and temperature robustness (no bias drift problem). The overall intrinsic loss of the modulator is ~3dB. The AOM was driven by arbitrarily shaped pulse waveforms in order to reduce the effects of pulse steepening in the fiber amplifier chain. In this effort, the leading edge of the pulse is pre-attenuated in order to compensate for the higher gain experienced by this edge. Figure 9 displays a sample waveform demonstrating this mentioned pre-distortion of the pulse, and how this pulse corrects through the power amplifier.

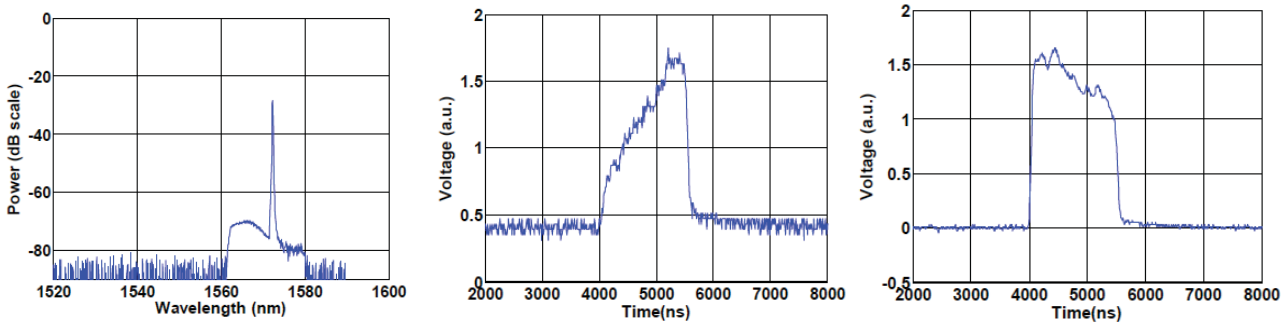

(a) (b) (c)

Figure 9. (a) Stage 1 EDFA output spectrum at 80 mW output; Measured waveform showing pre-distorted pulses to avoid pulse-steepening (b), after power amplifier (c).

The second stage EDFA is built with a highly Erbium doped, single mode PM gain fiber (7/125 μm core and cladding), and pumped with a telecom grade single mode frequency stabilized pump diode. This amplifier serve as a low energy preamplifier module for the stage 3 amplifier, and produces ~ 1 μJ energy at 10 kHz. The stage 3 EDFA is built with the same fiber that is used in stage 1 EDFA, and generates up to 40 μJ energy at 10 kHz.

The final power amplifier stage, EDFA 4, employed a commercial PM LMA fiber with 25 μm core diameter and 0.1 core numerical aperture (NA). Simple coiling of the gain fiber to ~12 cm diameter enabled single mode operation. The amplifier was counter-pumped by a tandem of 975 nm pump lasers, with up to 50 W of pump power coupled into the gain fiber through a custom PM fused fiber combiner. Another custom PM fused combiner with a built-in mode field adapter (from 9/125 μm to 25/300 μm) was placed at the input of the gain fiber along with 1% tap ports for forward and reverse Stimulated Brillouin Scattering (SBS) monitoring. The output passive delivery PM LMA fiber was terminated with a ~10% angle-cleave in order to reduce back reflections. The gain fiber was cooled with forced-air, and the pump diodes were mounted on a water-cooled base plate at 25°C. A longpass filter was placed at the output to clean up leakage pump light at 975 nm, and any ASE at the 1 μm band.

With this amplifier, and the ~1 MHz linewidth seed source, we were able to obtain up to ~156 µJ. The limit for this energy was the SBS threshold of the amplifier. We define the SBS threshold as when the backward scattered Brillouin spectral peak reaches the same relative intensity as the backward scattered Rayleigh spectral peak and these backward signals were continuously monitored with a 1% reverse tap coupler during the experiments using a high resolution OSA. When compared to the forward energy, this definition of SBS threshold is very conservative. In fact, our measurements show that, the absolute backscattered light (including Rayleigh and SBS light) is >40 dB below the forward energy with this SBS threshold definition.

The output optical spectrum at 156 µJ (with and without bandpass filter), backwards spectral plot, and output pulse shape plots are shown in Figure 10. The SBS peak is ~5dB above the Rayleigh peak, which is very slightly above SBS threshold.

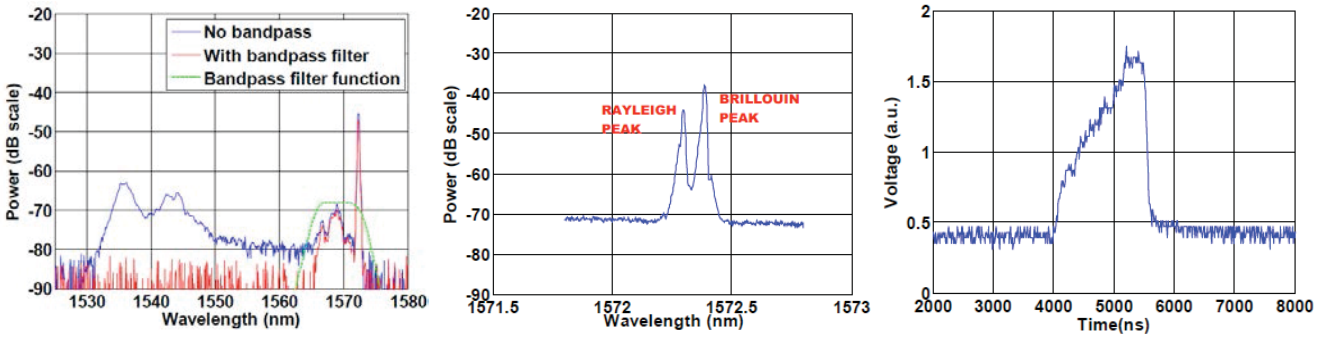

(a) (b) (c)

Figure 10. EDFA4 output at 1572.3 nm, 156 µJ, 10 kHz, ~1 MHz linewidth, ~1.4 µs pulsewidth. (a) Output optical spectrum with and without bandpass filter, (b) backward SBS spectrum, and (c) output pulse shape.

Normally SBS is the main limiting factor for coherent (single frequency) fiber amplifiers, where the usual peak power threshold (limit) is on the order of 100-200 Watts for LMA fibers. In order to mitigate SBS peak power limits, Fibertek utilized their proprietary techniques using rf photonics techniques to spectrally broaden the MO linewidth in a controlled manner, while maintaining the original coherence length of the seed laser. With this setup, multiple replicas of the original seed laser optical spectrum at the intervals corresponding to the rf frequency (optical frequency comb), with equal amplitudes can be generated. Therefore, the SBS threshold can be increased proportional to the number of equal-amplitude peaks (optical frequency combs) that are generated. The overall bandwidth of the signal is precisely determined by the ~1 MHz seed linewidth and the rf signal generator frequency that is usually accurate to the milliHertz level. The output signal can be described mathematically as the sum of individual ~1 MHz linewidth lasers that are linked precisely in optical frequency (by the fixed frequency separation) and phase. A single rf sinusoidal source can easily generate three equal amplitude frequency comb lines, as shown with a sample simulation in Figure 11(a). The simulations were done for a center frequency of ~190 THz (1572 nm) and RF frequency of 500 MHz for ease of computation. However, the shape of the optical spectra is independent of the absolute frequencies. For more comb lines, two or more RF sine wave sources can be combined with carefully selected frequencies and modulation indices as shown in Figure 11(b).

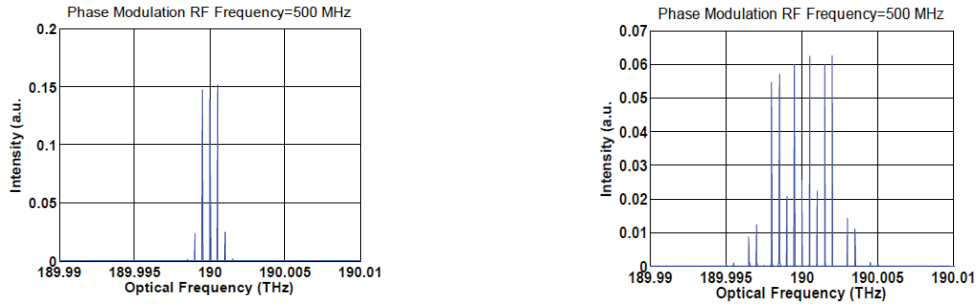

(a) (b)

Figure 11. Sample optical spectra with RF sinusoidal phase modulation (a) single 500 MHz rf tone, (b) two-tone 500 MHz and 1500 MHz

Using the broadening technique discussed above, we were able to achieve up to 300 µJ energy at 50 MHz total bandwidth, and up to 475 µJ energy at 100 MHz total bandwidth. The pulse was 1.5 µs in width and square with mild steepening that can be corrected with very small changes to the pre-distorted pulse that is fed into the AOM. The pump to signal optical to optical conversion efficiency was ~16.7% with respect to the total pump power (not absorbed pump or slope).

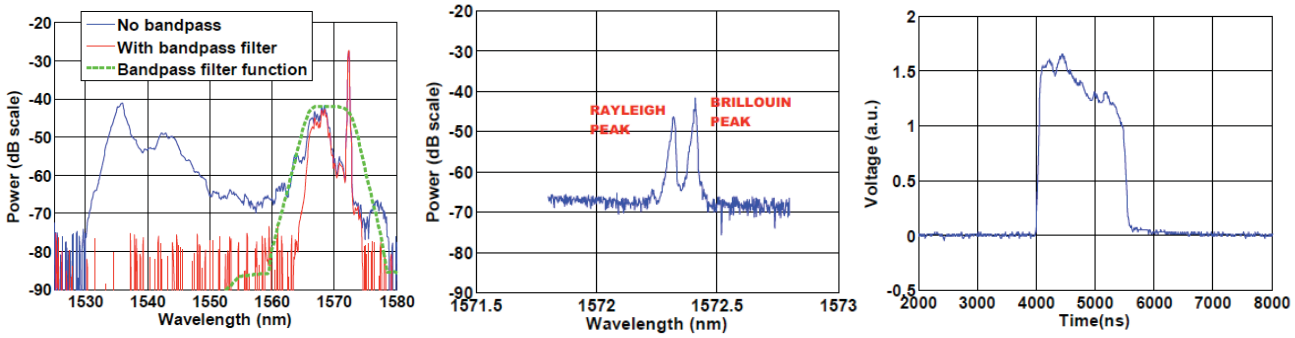

(a) (b) (c)

Figure 12. EDFA4 output at 1572.3 nm, 475 µJ, 10 kHz, ~100 MHz linewidth, ~1.5us pulsewidth. (a) Output optical spectrum with and without bandpass filter, (b) backward SBS spectrum, and (c) output pulse shape.

The output beam quality (after the bandpass filter) was measured at ~375 µJ energy with a Spiricon CCD (SP-1550-M). The beam was contained in a single transverse mode with M^2 estimated to be less than 1.2 in both directions. The PER of the output was also measured at 375 µJ energy by rotating a high-extinction ratio polarizer and recording the maximum and minimum readings on the meter. The PER was ~17.26 dB.

2.3.2.2 O_2 Channel – Power Scaling of 1529 nm

We conducted similar experiments as above at the center wavelength of 1529 nm. The EDFA1 to EDFA3 for 1529 nm was re-optimized by shortening the gain fiber lengths, while the EDFA4 power amplifier stage used in the 1572 nm case remained unchanged in order to keep the gain fiber intact for future possible experiments. The obtained energy levels at 1529 nm at each stage are illustrated in Figure 13.

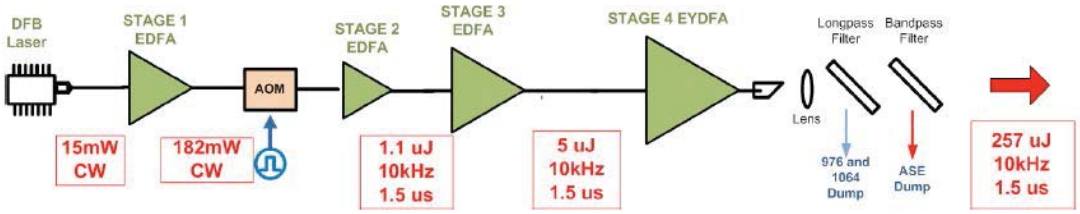

Figure 13. Experimental setup with illustrated 1529 nm power/energy levels at each stage

A DFB-LD with a center wavelength of ~1529 nm and output power of up to 15 mW was used and, as previous case, was operated in continuous-wave (CW) mode for best wavelength stability and narrowest linewidth of <1 MHz. The EDFA1 gain fiber was cut to ~6 meters, and up to 182 mW output average power was obtained at 1529 nm. There was a fiber-pigtailed 1529 nm filter at the output of the amplifier with ~ 3nm pass band to eliminate residual ASE.

For the pulse generation, the pre-distorted pulse waveform was adjusted due to different amplifier behavior at 1529 nm compared to 1572.3 nm. The second stage EDFA was kept the same as before, and produced ~ 1.1µJ energy at 10 kHz. The stage 3 EDFA gain fiber length was reduced also to ~6 meters, and obtained ~5 µJ from this stage, which limited the EDFA4 operation. For the output of EDFA4, we utilized a ~3nm FWHM passband filter centered at 1550 nm (at normal incidence). This filter was tilt tuned to ~1528 nm in order to clean up ASE peak at ~1535 nm. Due to the large tilt angle, higher loss (~20%) was introduced into the system at the signal wavelength. There is also a slight effect from the Er/Yb gain reduction for wavelengths beyond 1529 nm based on emission spectrum of the gain fiber.

As mentioned earlier, we kept the final power amplifier, EDFA 4, was in the same configuration as the 1572.3 nm experiments, only changing the output bandpass filter, and a small pump added to the forward direction. The reason for this small pumping is to have some gain at the first meter of the gain fiber, since the gain fiber is already too long for efficient 1529 nm amplification. With this amplifier, and the ~1 MHz linewidth 1529 nm seed source, we were able to obtain up to ~133 µJ signal energy at 10 kHz registered at the output of the bandpass filter. Considering the loss of the bandpass filter as mentioned earlier, and correcting for the residual ASE (based on OSA measurements), we calculate an output signal-only energy of ~161 µJ. The limit for this energy was the SBS threshold of the amplifier.

The output optical spectrum at 161 µJ (with and without bandpass filter), backwards spectral plot, and output pulse shape plots are shown in Figure 14. The FWHM is ~1.4 µs due to the non square shape. With slight modifications to the pre-distorted pulse, the output pulse can be turned into a square shape easily. The pump to signal optical to optical conversion efficiency was ~9% with respect to the total pump power (not absorbed pump or slope). This is lower than previous 1572.3 nm experiments, because the gain fiber length was not optimized for 1529 nm. Ideally, at 1529 nm, there is more potential to reach higher energies (compared to 1572.3 nm) due to the shorter gain fiber that is required.

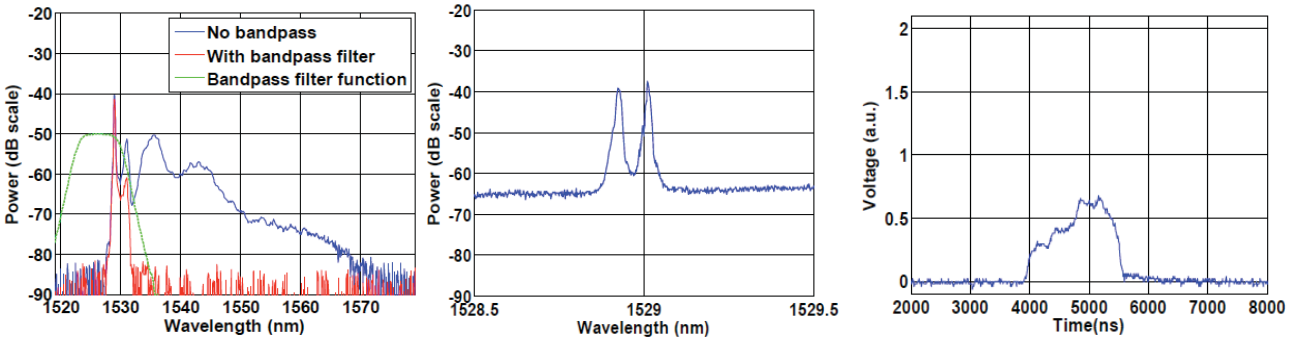

(a) (b) (c)

Figure 14. EDFA4 output at 1529 nm, 161 µJ, 10 kHz, ~1 MHz linewidth, ~1.4 µs pulsewidth. (a) Output optical spectrum with and without bandpass filter, (b) backward SBS spectrum, and (c) output pulse shape.

Using the broadening technique discussed earlier, we were able to achieve up to 257 µJ energy at 100 MHz total bandwidth (RF frequency of 50 MHz). The pulse was 1.5 µs in width and square with mild structure that can be corrected with very small changes to the pre-distorted pulse that is fed into the AOM. The pump to signal optical to optical conversion efficiency was again ~9% with respect to the total pump power (not absorbed pump or slope). The output beam quality (after the bandpass filter) was measured at the maximum 257 µJ energy and the beam was contained in a single transverse mode, with M^2 estimated to be less than 1.2 in both directions.

The PER of the output was also measured at 257 µJ energy by rotating a high-extinction ratio polarizer and recording the maximum and minimum readings on the meter. The PER was ~17 dB , and the real PER in the signal could be slightly higher due to the residual ASE influencing the measurement.

In summary, we have successfully demonstrated power scaling of the CO2 and O2 channels at 1572 nm and 1529 nm wavelengths. The table below summarizes the achieved energy levels with corresponding spectral linewidths.

Table 3. Summary of the fiber amplifier breadboard results showing the achieved pulse energy at the 1572 and 1529 nm wavelengths and 1 MHz and 100 MHz spectral widths.

Wavelength [nm]	Repetition Rate [kHz]	Pulse Width [µs]	Output Pulse Energy @ <1 MHz linewidth [µJ]	Output Pulse Energy @ 100 MHz linewidth [µJ]	Beam Quality, M^2	PER [dB]
1572.3	10	1.5	156	475	<1.2	17
1529	10	1.5	161	257	<1.2	17

CONCLUSIONS

We have made significant progress on developing a parallel approach in power scaling laser energies at appropriate wavelengths to meet the CO_2 and O_2 sensing from space. We are still awaiting the delivery of the PWG that meet our design parameters, preliminary results from thicker PWGs showed promising results. This multi-pass PWG approach will be beneficial to future space-based applications. For the multi-aperture case, we used fiber components from the telecommunication industry and have successfully demonstrated results at 1572.3 nm and 1529 nm that are several times better than the published results in the literature. We are working on a follow-on effort that will further develop the fiber amplifier approach that will have a direct path for space deployment.

ACKNOWLEDEMENT

The authors would like to acknowledge the financial support from NASA Earth Science Technology Office (ESTO) and NASA Goddard Space Flight Center Internal Research and Development (IRAD) program.

REFERENCES

1. NASA ASCENDS Mission Science Definition and Planning Workshop Report, Available from: http://cce.nasa.gov/ascends/12-30-08%20ASCENDS_Workshop_Report%20clean.pdf, 2008.
2. Abshire, J.B. et al., "A lidar approach to measure CO2 concentrations from space for the ASCENDS Mission," Proc. SPIE 7832, paper 78320D, November 2010, doi:10.1117/12.868567.
3. Kawa, S., et al., "Simulation studies for a space-based CO2 lidar mission," Tellus B, 62, Dec. 2011.
4. Abshire, J.B., et al. "Pulsed Airborne Lidar Measurements of Atmospheric CO_2 Column Absorption," Tellus Series B-Chemical And Physical Meteorology, 62 (5) pp. 770-783 (2010).
5. Amediek, A., et al., "Analysis of Range Measurements From a Pulsed Airborne CO_2 Integrated Path Differential Absorption Lidar," IEEE Trans Geosci. Rem. Sensing, vol. PP, no.99, pp.1-7, 2012, doi: 10.1109/TGRS.2012.2216884.
6. Stephen, M.A., et al., "Narrowband, tunable, frequency-doubled, erbium-doped fiber-amplified transmitter," Optics Letters, Vol. 32, No. 15, pages 2073-6 (2007).
7. Stephen, M.A., et al., "Oxygen Spectroscopy Laser Sounding Instrument for Remote Sensing of Atmospheric Pressure," IEEE Aerospace Conference, pages 1-6, doi: 10.1109/AERO.2008.4526388 (2008).
8. Measures, R., Laser Remote Sensing: Fundamentals and Applications, Krieger Publishing, New York (1992).
9. Abshire, J.B., et al., "Airborne measurements of CO_2 column absorption and range using a pulsed direct-detection integrated path differential absorption lidar," Appl. Opt. 52, 4446-4461 (2013).
10. Abshire, J.B., et al., "Pulsed airborne lidar measurements of CO_2 column absorption," NASA ESTO ESTF-2011 Conference (2011), avail from: http://esto.nasa.gov/conferences/estf2011/papers/Abshire_ESTF2011.pdf
11. Allan, G.R., et al., "Laser Sounder for Active Remote Sensing Measurements of CO2 Concentrations", IEEE Aerospace Conference, doi: 10.1109/AERO.2008.4526387, Page(s): 1 – 7, 2008.
12. Ehret, G., et al. "Space-borne remote sensing of CO2, CH4, and N2O by integrated path differential absorption lidar: A sensitivity analysis," Appl. Phys. B 90, 593–608, DOI: 10.1007/s00340-007-2892-3 (2008).
13. Champert, P.A., et al., "Power scalability to 6 W of 770 nm source based on seeded fibre amplifier and PPKTP," Electronics Letters 37 (18): 1127-1129 Aug. 30 (2001).
14. Wei, S., et al. "Kilowatt-level stimulated-Brillouin-scattering-threshold monolithic transform-limited 100 ns pulsed fiber laser at 1530 nm," Optics Letters 35(14) pp 2418-2420 (2010).
15. Numata, K., et al., "Frequency stabilization of distributed-feedback laser diodes at 1572 nm for lidar measurements of atmospheric carbon dioxide," Appl. Opt., 50, 1047-1056 (2011).
16. Numata, K., et al., "Precision and fast wavelength tuning of a dynamically phase-locked widely-tunable laser," Opt. Express, 20, 14234-14243 (2012).
17. Numata, K., et al., "Frequency stabilization of distributed-feedback laser diodes at 1572 nm for lidar measurements of atmospheric carbon dioxide," Applied Optics, 50, 7, 1047, (2011).

18. Yu, A.W. et al., "Highly Efficient Yb:YAG Master Oscillator Power Amplifier Laser Transmitter for Lidar Applications," in Conference on Lasers and Electro-Optics 2012, OSA Technical Digest (online), paper JTh1I.6, 2012.
19. Song, F. et al., “Spectra characteristics of novel Er:Yb phosphate glass.,” Proc. SPIE 3280, Rare-Earth-Doped Devices II, 46 (April 15, 1998); doi:10.1117/12.305406.
20. Filgas, D., et al., “Recent Results for the Raytheon RELI Program,” Laser Technology for Defense and Security VIII, edited by Mark Dubinskii, Stephen G. Post, Proc. of SPIE Vol. 8381 83810W, 2012. doi: 10.1117/12.921055.